Inter- and Intramolecular Photoinduced Electron-Transfer Processes between C_{60} and Diphenylaminofluorene in Solutions

Hongxia Luo,[†] Mamoru Fujitsuka,[†] Yasuyuki Araki,[†] Osamu Ito,*[,†] Prashant Padmawar,[‡] and Long Y. Chiang*[,‡,§]

Institute of Multidisciplinary Research for Advanced Materials, Tohoku University, CREST (JST), Katahira, Aoba-ku, Sendai, 980-8577 Japan, Center for Condensed Matter Sciences, National Taiwan University, Taipei, Taiwan, and Department of Chemistry, Institute of Nanoscience and Engineering, University of Massachusetts−Lowell, 265 Riverside Street, Lowell, Massachusetts 01854-5047

Received: March 18, 2003; In Final Form: May 28, 2003

Intramolecular photoinduced charge-separation and charge-recombination processes of a covalently bonded buckminsterfullerene−diphenylaminofluorene (C_{60}−DPAF) dyad, in which the diphenylaminofluorene moiety is connected to C_{60} via a ketone group, have been investigated. Quenching of the fluorescence intensities and the observed short fluorescence lifetimes of the C_{60} moiety of the dyad in benzonitrile (PhCN) and DMF indicated that charge separation takes place via the singlet excited state of the C_{60} moiety at a fast rate with high efficiency. On the basis of the nanosecond transient absorption spectra, formation of the radical ion pair $C_{60}^{\bullet-}$-$DPAF^{\bullet+}$ was confirmed in DMF; the radical ion pair decays with a lifetime of 150 ns. From the temperature dependence of the charge-recombination rate constants, the reorganization energy was evaluated to be 0.81 eV in DMF, which is reasonably small, characteristic of fullerene derivatives. On the other hand, a mixture of DPAF and C_{60} showed intermolecular electron transfer via the triplet state of C_{60} in polar solvents such as PhCN.

Introduction

Buckminsterfullerene (C_{60}) as a highly efficient electron acceptor exhibiting unique photophysical and electrochemical properties has attracted various researchers in recent years to develop the syntheses of the C_{60} derivatives including covalently linked electron donors.[1,2] In contrast to the simple mixture systems of C_{60} and the donors,[3] such dyad molecules are of particular interest in their ground and excited electronic states,[4] which makes them promising candidates for efficient photoinduced electron-transfer systems.[5] These phenomena enhance potential applications in relation to artificial photosynthetic systems, molecular electronic devices, and photovoltaic cells.[6] In the case of intramolecular photoinduced processes involving electron transfer between both electroactive entities, the excited singlet state of the C_{60} moiety can act as an electron-accepting component of such devices due to the high electronegativity arising from its unique spherical π-electron system.

Among a wide variety of donor molecules available for linking covalently to C_{60}, commonly used ones were electron-rich tertiary amines such as dimethylaniline.[7] In our previous study of the fullerene dyad, we demonstrated the effect of the bis(biphenyl)aminophenyl moiety on prolonging the lifetime of the radical ion pair in polar solvents such as benzonitrile (PhCN).[8] Similarly, a related tertiary amino derivative, diphenylaminofluorene (Scheme 1),[9] was covalently linked to the C_{60} molecule through a spacer, with the expectation of efficient photoinduced charge separation. In the present paper, the photoinduced charge separation and lifetime of the radical ion pair of the new dyad have been investigated by laser flash photolysis methods. For comparison, intermolecular electron transfer between diphenylaminofluorene derivatives and C_{60}, which proceeds via the excited triplet state of C_{60}, has also been studied in this paper.

SCHEME 1: Molecular Structures

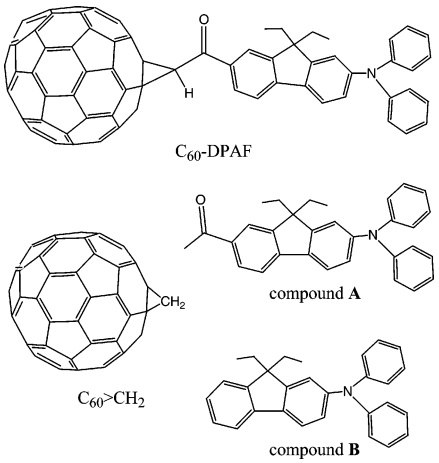

Experimental Section

Materials. 7-Acetyl-9,9-diethyl-2-diphenylaminofluorene (compound **A**), 9,9-diethyl-2-diphenylaminofluorene (compound **B**), and 7-(1,2-methano[60]fullerene-61-carbonyl)-9,9-diethyl-2-diphenylaminofluorene (C_{60}−DPAF) were synthesized by the method described previously.[9] Pure C_{60} (99.5% purity) was obtained from MER Corp. Reagents and solvents were purchased as reagent grade and used without further purification.

Measurements. *Electrochemical Measurements.* Cyclic voltammograms were obtained using a conventional three-electrode

* To whom correspondence should be addressed. E-mail: ito@tagen.tohoku.ac.jp (O.I.); Long-Chiang@uml.edu (L.Y.C.).
[†] Tohoku University.
[‡] National Taiwan University.
[§] University of Massachusetts−Lowell.

10.1021/jp034689g CCC: $25.00
Published on Web 08/06/2003

system with a BAS CV-50W potentiostat/galvanostat. A platinum disk electrode (1 mm in diameter) was used as a working electrode. A platinum wire served as a counter electrode. An Ag/AgCl electrode was used as the reference electrode. The potentials were referenced to an internal ferrocene/ferrocenium (Fc/Fc^+) redox couple.

Steady-State Measurements. Steady-state absorption spectra in the visible and near-IR regions were measured on a JASCO V570 DS spectrophotometer. Steady-state fluorescence spectra were measured on a Shimadzu RF-5300 PC spectrofluorophotometer equipped with a photomultiplier tube having high sensitivity up to 800 nm.

Time-resolved Fluorescence Measurements. The time-resolved fluorescence spectra were measured by a single-photon counting method using second harmonic generation (SHG; 410 nm) of a Ti:sapphire laser (Spectra-Physics, Tsunami 3950-L2S, 1.5 ps fwhm) and a streakscope (Hamamatsu Photonics, C4334-01) equipped with a polychromator (Acton Research, SpectraPro 150) as the excitation source and detector, respectively.[10] Lifetimes were evaluated with the software attached to the equipment.

Nanosecond Transient Absorption Measurements. Nanosecond transient absorption measurements were carried out using SHG (532 nm) of a Nd:YAG laser (Spectra-Physics, Quanta-Ray GCR-130, 6 ns fwhm) as the excitation source. For transient absorption spectra in the near-IR region (600−1200 nm) and the time profiles, monitoring light from a pulsed Xe lamp was detected with a Ge-APD (Hamamatsu Photonics, B2834).[10] For spectra in the visible and near-IR regions (400−1000 nm), an Si-PIN photodiode (Hamamatsu Photonics, S1722-02) was used as the detector.[10] All the samples in a quartz cell (1 × 1 cm) were deaerated by bubbling argon through the solution for 10 min.

Molecular Orbital Calculations. The optimized structure, energy levels of the molecular orbitals, and electron densities of the HOMO and LUMO were calculated by GAUSSIAN 98 (HF/3-21G level).

Results and Discussion

Intermolecular Electron Transfer in a Polar Solvent. Figure 1 shows the cyclic voltammograms of **A**, **B**, and C_{60}−DPAF in benzonitrile (PhCN). For compounds **A** and **B**, pairs of reversible redox waves were observed, from which the oxidation potentials (E_{ox}) were evaluated to be 0.48 and 0.42 V vs Fc/Fc^+, respectively. The ketone group slightly increases the E_{ox} value, decreasing the electron-donor ability. Free-energy changes for intermolecular electron transfer (ΔG_{et}^T) from **A** or **B** to the triplet state of C_{60} ($^3C_{60}$*) were calculated by eq 1,[11]

$$\Delta G_{et}^{T} = E_{ox}(\mathbf{A} \text{ or } \mathbf{B}) - E_{red}(C_{60}) - E_T(C_{60}) - E_c \quad (1)$$

where $E_{red}(C_{60})$ is the reduction potential of C_{60} (−0.93 V vs Fc/Fc^+),[12] $E_T(C_{60})$ is the T_1 energy level (1.51 eV),[13] and E_c is the Coulombic energy (0.06 eV in PhCN).[3a] As listed in Table 1, sufficiently negative ΔG_{et}^T values predict diffusion-controlled second-order rate constants for the electron-transfer processes via $^3C_{60}$* in PhCN.

Steady-State Absorption Measurements. Steady-state absorption spectra of C_{60} and compounds **A** and **B** in PhCN are shown in Figure 2. The absorption spectra of the mixtures of C_{60} with **A** or **B** are almost identical with the corresponding added spectra of the constitutes, suggesting no appreciable interaction in the ground state. On employing the 532 nm laser light as an excitation source, C_{60} was predominantly excited in the nanosecond transient absorption measurements.

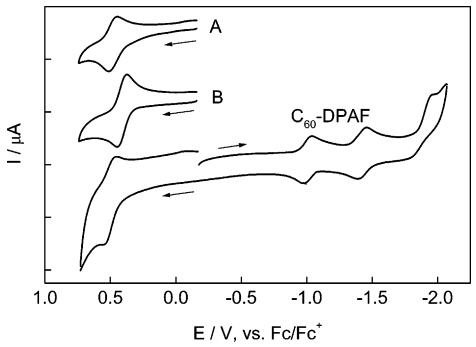

Figure 1. Cyclic voltammograms of **A** (0.1 mM), **B** (0.1 mM), and C_{60}−DPAF in PhCN containing 0.05 M Bu_4NClO_4 as the supporting electrolyte at a scan rate of 0.1 V s^{-1}.

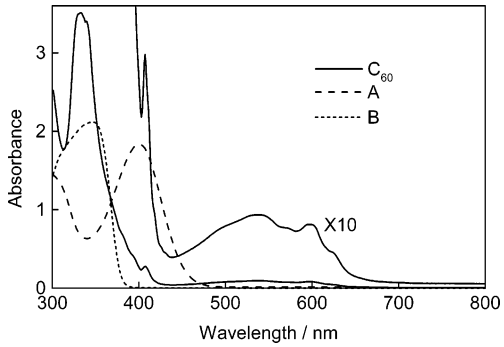

Figure 2. Steady-state absorption spectra of C_{60} (0.1 mM), **A** (0.1 mM), and **B** (0.1 mM) in PhCN.

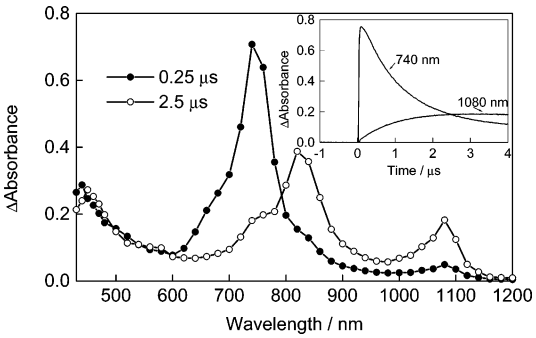

Figure 3. Nanosecond transient absorption spectra of C_{60} (0.1 mM) in the presence of **A** (0.5 mM) in PhCN after 532 nm laser irradiation. Inset: time profiles of absorbance at 740 and 1080 nm.

TABLE 1: Oxidation Potentials (E_{ox}) of Donors, Free-Energy Changes (ΔG_{et}^T), Quenching Rate Constants (k_q^T), Quantum Yields (Φ_{et}^T), and Electron-Transfer Rate Constants (k_{et}^T) via $^3C_{60}$* in PhCN

	E_{ox}/V	ΔG_{et}^T/eV	$k_q^T/M^{-1}\,s^{-1}$	Φ_{et}^T	$k_{et}^T/M^{-1}\,s^{-1}$
compound **A**	0.48	−0.16	1.1×10^9	0.45	0.50×10^9
compound **B**	0.42	−0.22	1.5×10^9	0.55	0.83×10^9
aminofluorene	0.25	−0.39	4.0×10^9	0.62	2.50×10^9
$(Ph)_3N$	0.40	−0.24	1.3×10^9	0.63	0.82×10^9

Nanosecond Transient Absorption Measurements. Transient absorption spectra observed by the nanosecond laser excitation (532 nm) of C_{60} in the presence of **A** in PhCN are shown in Figure 3. Immediately after the laser pulse, a transient absorption band appeared at 740 nm, which was ascribed to the excited triplet state of C_{60} ($^3C_{60}$*).[3] The absorption intensity of $^3C_{60}$* decayed with a concomitant increase of two absorption bands at 820 and 1080 nm, which were attributed to the radical cation

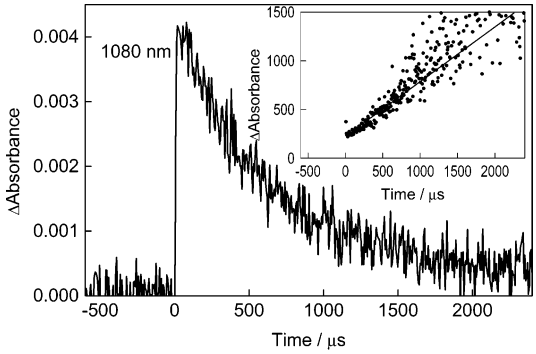

Figure 4. Decay of the radical anion of C_{60} at 1080 nm in a mixture of **A** (0.2 mM) and C_{60} (0.1 mM) in PhCN after 532 nm laser irradiation. Inset: second-order plot.

of **A** ($\mathbf{A}^{\bullet+}$) and the radical anion of C_{60} ($C_{60}^{\bullet-}$), respectively.[14] As shown in the inset of Figure 3, the time profile at 1080 nm showed an increase almost as a mirror image of the decay profile of $^3C_{60}$*, indicating that intermolecular electron transfer takes place via $^3C_{60}$* by accepting an electron from **A**, as shown in eq 2. In the case of **B**, similar transient spectra and time profiles were observed.

$$^3C_{60}^* + \mathbf{A/B} \xrightarrow[k_{et},\,\Phi_{et}]{k_q} C_{60}^{\bullet-} + A^{\bullet+}/B^{\bullet+} \qquad (2)$$

Each decay profile obeys first-order kinetics, giving the rate constant $k_{\text{first-order}}$, which increases with the concentration of **A** or **B**. The pseudo-first-order plots of $k_{\text{first-order}}$ vs [**A**] or [**B**] give the second-order rate constant for the quenching of $^3C_{60}$* (k_q^T) as 1.1×10^9 and 1.5×10^9 M^{-1} s^{-1}, respectively. The efficiency of electron transfer can be evaluated from the ratio of the maximal concentration of $C_{60}^{\bullet-}$ ($[C_{60}^{\bullet-}]_{max}$) to the initial concentration of $^3C_{60}$* ($[^3C_{60}^*]_{init}$), which were evaluated from the intensities of the observed absorbances and reported molar extinction coefficients (16100 M^{-1} cm^{-1} for $^3C_{60}$* at 740 nm[15] and 12100 M^{-1} cm^{-1} for $C_{60}^{\bullet-}$ at 1080 nm[3b]). The plot of $[C_{60}^{\bullet-}]_{max}/[^3C_{60}^*]_{init}$ vs [**A**] or [**B**] shows saturation at higher concentrations than 2 mM. The saturated value can be regarded as equivalent to the quantum yield (Φ_{et}^T) of electron transfer via $^3C_{60}$*;[16] thus, the Φ_{et}^T values were evaluated to be 0.45 and 0.55 for **A** and **B**, respectively, and the electron-transfer rate constants (k_{et}^T) were finally evaluated to be 5.0×10^8 and 8.3×10^8 M^{-1} s^{-1}, respectively, from the relationship $k_{et}^T = \Phi_{et}^T k_q^T$. As compared with the k_{et}^T value between $^3C_{60}$* and 2-aminofluorene, which showed the largest k_{et}^T value as listed in Table 1, compounds **A** and **B** showed relatively less electron donating abilities in the intermolecular electron-transfer processes, probably due to sterical reasons around the N atom. The k_{et}^T value of **B** is slightly higher than that of **A**, probably due to the electron-withdrawing property of the acetyl group of **A** in reducing the electron density of the DPAF moiety as evidenced from a slightly higher E_{ox} value of **A** than that of **B**. Triphenylamine having an E_{ox} value similar to that of **B** showed a k_{et}^T value similar to that of **B**.[17] Extended electron delocalizations in the radical cations generated in **A** and **B** are evident as the corresponding optical absorption bands appeared at longer wavelengths (>800 nm) than those of 2-aminofluorene and triphenylamine at 600 nm.[17]

Absorption intensities of the radical ions began to decay after the maxima at 5−10 μs were reached, as shown in the time profiles on a long time scale (Figure 4). The decay profile obeys second-order kinetics as depicted in the inset of Figure 4. Such second-order kinetics indicates that back electron transfer (k_{bet})

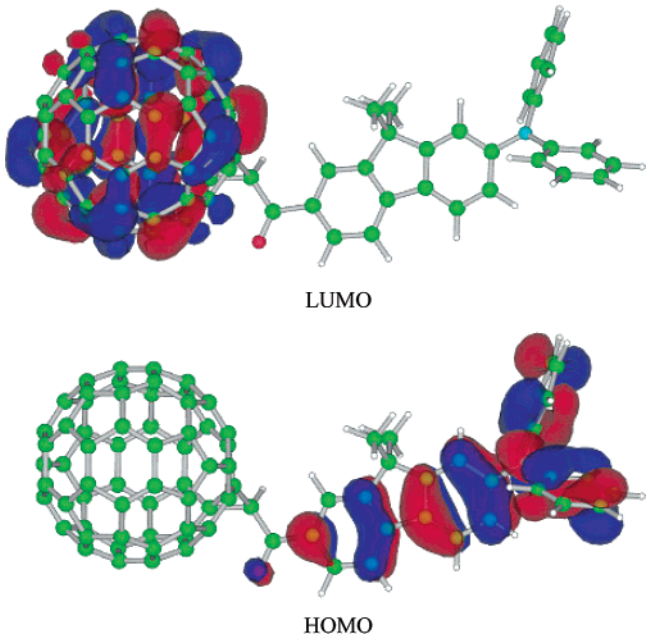

Figure 5. Molecular orbitals of C_{60}−DPAF.

takes place from $C_{60}^{\bullet-}$ to $\mathbf{A}^{\bullet+}$ or $\mathbf{B}^{\bullet+}$ after each radical ion is separately solvated as an individual free radical ion (eq 3).[18]

$$(C_{60}^{\bullet-})_{solv} + (\mathbf{A}^{\bullet+}/\mathbf{B}^{\bullet+})_{solv} \xrightarrow{k_{bet}} C_{60} + \mathbf{A/B} \qquad (3)$$

The slope of the second-order plot corresponds to the ratio of k_{bet} to the molar extinction coefficient of the radical ions. The k_{bet} values were found to be 7.5×10^9 and 1.5×10^{10} M^{-1} s^{-1} in PhCN for $\mathbf{A}^{\bullet+}$ and $\mathbf{B}^{\bullet+}$, respectively.

Intramolecular Electron Transfer in Polar Solvent. *Molecular Orbital Calculations.* The optimized structure of the C_{60}−DPAF dyad calculated using GAUSSIAN 98 (HF/3-21G level) is shown in Figure 5 with electron densities of the HOMO and LUMO. The energy minimal structure consists of the DPAF moiety in a normal direction with respect to the C_{60} sphere, revealing a negligible electronic interaction between DPAF and C_{60}; two phenyl moieties of the diphenylamino (DPA) group are also found to be perpendicular to the fluorene plane. From the HOMO, the center of the electron density of DPAF locates on the phenyl ring of fluorene linked to the N atom; thus, the center-to-center distance between C_{60} and DPAF was estimated to be 13 Å (Figure 5).

The electron density of the HOMO showed delocalization over the whole DPAF moiety; high electron density was observed on the DPA moiety. On the contrary, only a relatively small electron density was found on the carbonyl oxygen atom. In the case of the LUMO, the electron density is predominantly localized on the C_{60} moiety. This suggests that the first oxidation is attributed to the DPAF moiety, while the first reduction wave is ascribed to the C_{60} moiety. Accordingly, in the charge-separation state of C_{60}−DPAF, the HOMO electron density pattern corresponds to the hole distribution, while the LUMO pattern corresponds to the electron distribution.

Electrochemical Measurements. Cyclic voltammograms of C_{60}−DPAF displayed an almost reversible pattern of redox waves (Figure 1), from which the E_{ox} value was found to be 0.50 V vs Fc/Fc^+ in close resemblance to that of **A**. This revealed a good correlation of the E_{ox} value of C_{60}−DPAF with that of the DPAF moiety. Similarly, the first E_{red} value of C_{60}−DPAF was evaluated to be −1.00 V vs Fc/Fc^+, which is slightly negative of that of pristine C_{60} (E_{red} = −0.93 vs Fc/Fc^+). Thus,

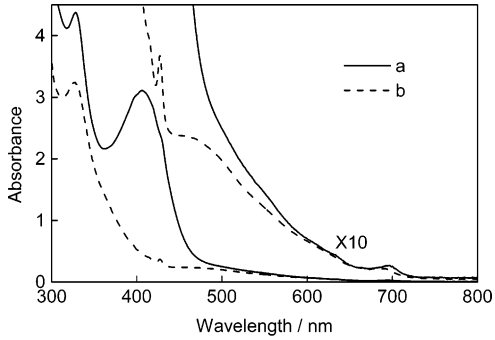

Figure 6. Steady-state absorption spectra of (a) C_{60}−DPAF (0.1 mM) and (b) methanofullerene (0.1 mM) in PhCN.

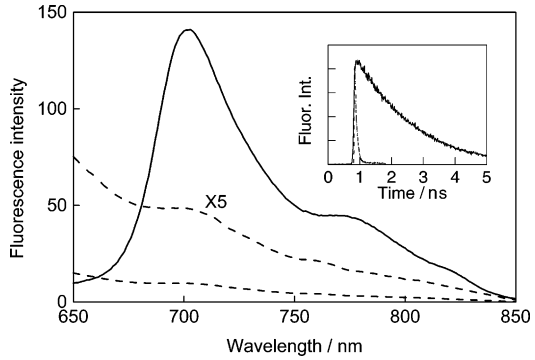

Figure 7. Steady-state fluorescence spectra of C_{60}−DPAF (0.1 mM) in (a) toluene and (b) PhCN with excitation at 410 nm. Inset: time profiles at 700−730 nm.

it is reasonable to conclude that the observed E_{red} of the dyad corresponds to the reduction of the C_{60} moiety.

Steady-State Absorption Measurements. Steady-state absorption spectra of C_{60}−DPAF and methanofullerene (C_{60}>CH_2) in toluene are shown in Figure 6. The broad band at 700 nm is characteristics of C_{60}>CH_2 containing 58 conjugated π-electrons.[8] On the other hand, the absorption band in the region of 370−470 nm with a peak at 420 nm was attributed to the DPAF moiety (Figure 2). The absorption intensities of C_{60}−DPAF are found to fit approximately with the sum of the spectral intensities of C_{60}>CH_2 and DPAF, revealing negligible interaction between the C_{60} and DPAF moieties in the ground state. This finding is in good agreement with the electron distribution of the HOMO localizing on the DPAF moiety. Intramolecular charge-transfer transition from the HOMO (the DPAF moiety) to the LUMO (the C_{60} moiety) is expected to appear in the absorption spectrum in the wavelength region longer than 700 nm. However, no absorption was found in the wavelength region longer than 720 nm, suggesting weak interaction due to the molecular structure of C_{60}−DPAF, in which the DPAF moiety is in almost a normal position to the C_{60} moiety. Since the DPAF moiety absorbs light at wavelengths shorter than 470 nm, irradiation of C_{60}−DPAF with light of wavelength longer than 500 nm predominantly excites the C_{60} moiety.

Steady-State Fluorescence Measurement. The steady-state fluorescence spectrum of C_{60}−DPAF in toluene exhibits a fluorescence band (λ_f) centered at 452 and 714 nm when 410 nm light is used for excitation (Figure 7). The spectral shape and intensity at 714 nm were found to be almost the same as those of C_{60}>CH_2 in toluene (λ_f = 717 nm), suggesting that the origin of the observed fluorescence at 714 nm is the C_{60} moiety**.** On the basis of the fluorescence peak at 714 nm, the lowest excited singlet energy of $^1C_{60}$*−DPAF was estimated to be 1.74 eV. The 452 nm fluorescence was attributed to the

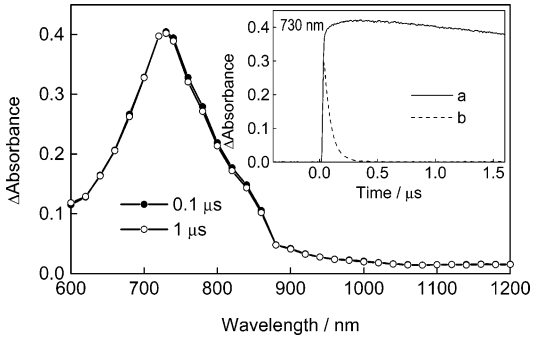

Figure 8. Nanosecond transient absorption spectra of C_{60}−DPAF (0.1 mM) in toluene after 532 nm laser irradiation. Inset: time profiles of absorbance in (a) argon-saturated toluene and (b) oxygen-saturated toluene at 730 nm.

DPAF moiety by comparison with the fluorescence of **A**, indicating the lowest excited singlet energy of C_{60}−^{1}DPAF* is 2.74 eV.

In polar solvents such as PhCN, fluorescence intensities of C_{60}−DPAF that at a wavelength longer than 680 nm decreased as shown in Figure 7. Such a decrease may indicate the occurrence of charge separation via the $^1C_{60}$* moiety. In DMF, appreciable fluorescence was not observed for C_{60}−DPAF, suggesting further efficient charge separation.

Fluorescence Lifetimes. Time profiles of the fluorescence intensity at the peak position of the $^1C_{60}$* moiety of C_{60}−DPAF in toluene and PhCN are displayed in the inset of Figure 7; in toluene, the fluorescence lifetime (τ_f) was evaluated from a decay curve obeying a single exponential to be τ_f = 1500 ps, which is close to τ_f = 1490 ps for C_{60}>CH_2.[8] A short fluorescence lifetime (τ_f = 60 ps) of C_{60}−DPAF in PhCN was observed in contrast to a long τ_f value in toluene. The fluorescence lifetime of $^1C_{60}$*−DPAF in PhCN did not show appreciable temperature change. In DMF, fluorescence decayed rapidly within the detector response limit (<20 ps); thus, the τ_f value may be shorter than 20 ps.

The shorter τ_f value of the $^1C_{60}$* moiety of C_{60}−DPAF in polar solvents than that in nonpolar solvent can be attributed predominantly to charge separation via the $^1C_{60}$* moiety, since the energy transfer from the $^1C_{60}$* moiety to the ground-state DPAF moiety is energetically improbable. Accordingly, intramolecular charge separation is proposed to occur from the DPAF moiety to the $^1C_{60}$* moiety, forming the corresponding radical ion pair ($C_{60}^{\bullet-}$−$DPAF^{\bullet+}$) in polar solvents.

From the measured τ_f values, the intramolecular charge-separation rate constant (k_{cs}) of C_{60}−DPAF in PhCN was calculated to be 1.6×10^{10} s^{-1} from the relationship $k_{cs} = (1/\tau_{f,sample} - 1/\tau_{f,reference})$.[7,8,19] This value indicated a rather fast charge separation comparable to those of other C_{60}−amine donor dyads in polar solvents.[7,8,19] The corresponding quantum yield of charge separation (Φ_{cs}) was subsequently evaluated from the equation $\Phi_{cs} = (1/\tau_{f,sample} - 1/\tau_{f,reference})/(1/\tau_{f,sample})$.[7,8,20] The resulting value of Φ_{cs} = 0.96 indicated clearly an efficient charge-separation process in PhCN. In DMF, the k_{cs} and Φ_{cs} values were evaluated to be $>5.0 \times 10^{10}$ s^{-1} and >0.99, respectively.

The fluorescence lifetimes of the ^{1}DPAF* moiety of C_{60}−DPAF were almost the same as those of **A** in toluene, PhCN, and DMF, suggesting that charge separation does not occur via C_{60}−^{1}DPAF*.

Nanosecond Transient Absorption Measurements. Transient absorption spectra of C_{60}−DPAF in toluene observed under nanosecond laser excitation at 532 nm are shown in Figure 8.

TABLE 2: Fluorescence Lifetimes (τ_f), Free-Energy Changes (ΔG_{CS}^S), Charge-Separation Rate Constants (k_{CS}^S), and Quantum Yields (Φ_{CS}^S) for Charge-Separation and Charge-Recombination Rate Constants (k_{CR}^S) of C_{60}−DPAF

	ΔG_{CS}^S/eV	τ_f/ps	k_{CS}^S/M^{-1} s^{-1}	Φ_{CS}^S	k_{CR}^S/M^{-1} s^{-1}
DMF	−0.29	<20	$>5 \times 10^{10}$	>0.99	6.7×10^6
PhCN	−0.27	60	1.6×10^{10}	0.96	
toluene	0.27	1500			

[a] $k_{CS} = 1/\tau_{f,sample} - 1/\tau_{f,reference}$ as $\tau_{f,reference} = 1.5$ ns. [b] $\Phi_{CS} = (1/\tau_{f,sample} - 1/\tau_{f,reference})/(1/\tau_{sample})$. [c] $-\Delta G_{CS} = \Delta E_{0-0} - E_{ox} + E_{red} - \Delta G_S$, where $\Delta G_S = e^2/(4\pi\Delta\epsilon_0)[(1/2R_+ + 1/2R_- - 1/R_{cc})1/\epsilon_s - (1/2R_+ + 1/2R_-)1/\epsilon_r]$, ΔE_{0-0} is the energy of the 0−0 transition of C_{60} (1.73 eV), E_{ox} (0.50 V vs Fc/Fc$^+$) and E_{red} (−1.00 V vs Fc/Fc$^+$) are the first oxidation potential of the donor and the first reduction potential of the acceptor in PhCN, respectively, R_+ and R_- are radii of the ion radicals of DPAF (7.6 Å) and C_{60} (4.7 Å), respectively, R_{cc} is the center-to-center distance between the two moieties (13 Å), and ϵ_s and ϵ_r are the static dielectric constants of the solvents used for the rate measurements and the redox potential measurements, respectively.

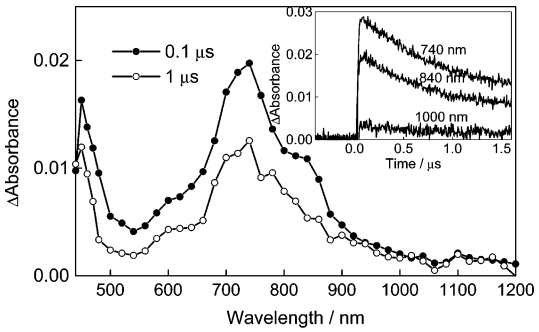

Figure 9. Nanosecond transient absorption spectra of C_{60}−DPAF (0.1 mM) in PhCN after 532 nm laser irradiation. Inset: time profiles of absorbance at 740, 840, and 1000 nm.

Only absorption of the $^3C_{60}$* moiety was detected at 730 nm.[8] The decay of this band is very slow, while the decay rate can be largely accelerated upon the addition of O_2 (inset of Figure 8), which indicated energy transfer from the $^3C_{60}$* moiety to O_2, producing singlet oxygen. These observations all support the formation of $^3C_{60}$*−DPAF in toluene. From the long-time decay measurement of the time profile, the lifetime of $^3C_{60}$*−DPAF was evaluated to be 33 μs, which is almost the same as that of $^3C_{60}$>CH_2* (35 μs).[8] This indicates that the intersystem crossing process from $^1C_{60}$*−DPAF to $^3C_{60}$*−DPAF is the predominant one with no charge separation; this finding can be rationalized by the positive free energy of charge separation via $^1C_{60}$*−DPAF ($\Delta G_{CS}^S = 0.27$ eV in toluene in Table 2). These considerations are also supported by the high fluorescence intensity and long fluorescence lifetime of the $^1C_{60}$* moiety in toluene.

Transient absorption spectra of C_{60}−DPAF in PhCN observed by nanosecond laser excitation (532 nm) are shown in Figure 9. The main absorption band around 740 nm of the $^3C_{60}$* moiety was observed immediately after the laser pulse. A weak transient absorption band appeared at 840 nm as a shoulder of the main absorption at 740 nm and may be attributed to the DPAF$^{\bullet+}$ moiety. However, the absorption band of the $C_{60}^{\bullet-}$ moiety was not clearly observed. The decay rates at 840 and 1000 nm (inset of Figure 9) were almost the same as that of the $^3C_{60}$* moiety at 740 nm, indicating that the decay of $C_{60}^{\bullet-}$-DPAF$^{\bullet+}$ was not clearly recognized in the time profiles, probably because the lifetime of $C_{60}^{\bullet-}$-DPAF$^{\bullet+}$ is too short for it to be observed by the nanosecond transient absorption method.

Transient absorption spectra of C_{60}−DPAF in DMF observed by nanosecond laser excitation (532 nm) are shown in Figure 10. Two main absorption bands were observed around 840 and 1000 nm corresponding to the DPAF$^{\bullet+}$ and $C_{60}^{\bullet-}$ moieties, respectively. The absorption band of the $^3C_{60}$* moiety did not appear in the spectra in DMF. As shown in the inset of Figure 10, the 840 nm band appeared immediately after the irradiation of the nanosecond laser pulse (fwhm = 6 ns), indicating that the charge-separation process takes place via the $^1C_{60}$* moiety, not via the $^3C_{60}$* moiety of C_{60}−DPAF. From the decay rate of the band centered at 840 nm, the rate constant for charge recombination (k_{CR}) was evaluated to be 6.7×10^6 s^{-1}, which corresponds to the lifetime of the charge-separated state (τ_{IP} = 150 ns). This decay rate increased sharply on the addition of O_2. On the basis of the fact that the DPAF$^{\bullet+}$ and $C_{60}^{\bullet-}$ moieties are not reactive to O_2,[20] this O_2 effect suggests that $C_{60}^{\bullet-}$-DPAF$^{\bullet+}$ has triplet-spin-state character highly sensitive to the triplet-state quencher, O_2.

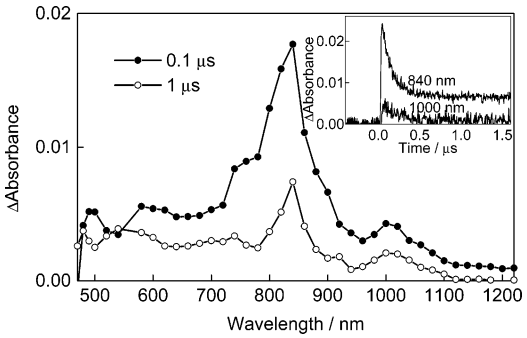

Figure 10. Nanosecond transient absorption spectra of C_{60}−DPAF (0.1 mM) in DMF after 532 nm laser irradiation. Inset: time profiles of absorbance at 840 and 1000 nm.

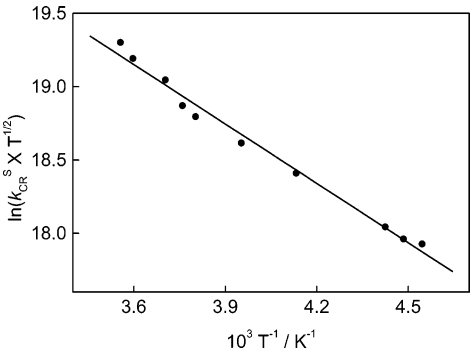

Figure 11. Modified Arrhenius plots for the temperature-dependent k_{CR}^S for C_{60}−DPAF (0.1 mM) in deaerated DMF.

Temperature Change of Decay Rates in DMF. The estimated k_{CR} values were found to be temperature dependent. From an Arrhenius plot, the activation energy for charge recombination was evaluated to be 0.11 eV in DMF, which implies that charge recombination of $C_{60}^{\bullet-}$-DPAF$^{\bullet+}$ occurs by leaping a considerable barrier. Plots of the k_{CR} values according to the semiclassical Marcus theory (eq 4,[21] where h, k_B, and T are the Boltzman

$$k_{CR}^S = (4\pi^3/h\lambda k_B T)^{1/2} V^2 \exp[-(\Delta G_{ET} + \lambda)^2/4\lambda k_B T] \quad (4)$$

constant, the Planck constant, and the absolute temperature, respectively) resulted in a straight line, as shown in Figure 11. From the slope and intercept, the electronic coupling matrix element (V) and reorganization energy (λ) in DMF were calculated to be 2.1 cm^{-1} and 0.81 eV, respectively. The λ value of 0.81 eV seems to be adequate for the C_{60}−donor dyads, since it is similar to the reported value for the C_{60}−zinc dyad (λ = 0.66 eV) in PhCN.[22] The V value of the present dyad was also

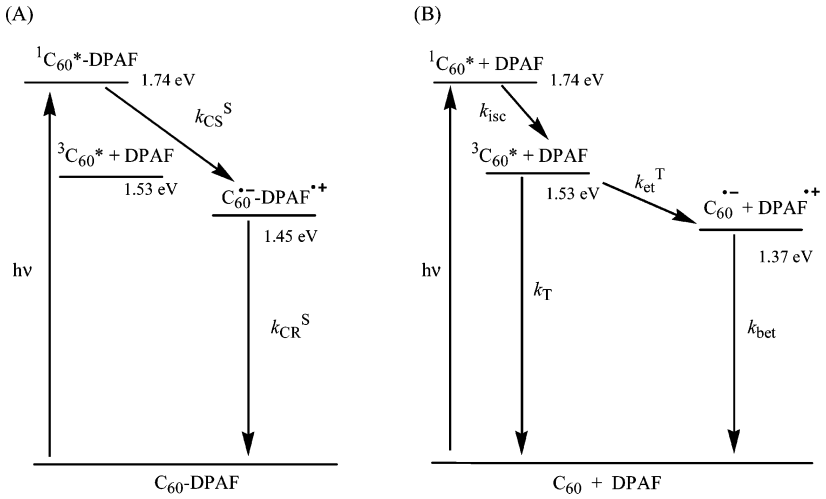

Figure 12. Energy diagrams for (A) C_{60}−DPAF in DMF and (B) a mixture of C_{60} and DPAF in PhCN.

similar to that of the C_{60}−zinc dyad (V = 3.9 cm^{-1}),[22] which may be appropriate for the observed k_{CR} value on the order of 10^6 s^{-1}.

Energy Diagrams. The short fluorescence lifetime of the $^1C_{60}$* moiety indicates that charge separation takes place via the $^1C_{60}$* moiety of C_{60}−DPAF, whose energy level was estimated to be 1.74 eV from the maximum of the fluorescence peak. ΔG_{CS}^S via the $^1C_{60}$* moiety can be estimated to be −0.29 eV in DMF (Table 2). The overall energy level diagram of C_{60}−DPAF in DMF can be illustrated as shown in Figure 12A. The 532 nm laser excitation pumps C_{60}−DPAF up from the ground state to $^1C_{60}$*−DPAF, from which charge separation takes place quite efficiently in DMF. Charge separation seems to be adequate from the fact that the energy level of $C_{60}^{\bullet-}$-DPAF$^{\bullet+}$ in DMF is lower than that of $^1C_{60}$*−DPAF, as indicated by the negative ΔG_{CS}^S value (Table 2). Subsequently, charge recombination of $C_{60}^{\bullet-}$-DPAF$^{\bullet+}$ occurs back to its ground state, since the energy level of $C_{60}^{\bullet-}$-DPAF$^{\bullet+}$ is lower than that of $^3C_{60}$*−DPAF in DMF.

In toluene, the energy level of $C_{60}^{\bullet-}$-DPAF$^{\bullet+}$ becomes higher than that of $^1C_{60}$*−DPAF as indicated by the positive ΔG_{CS}^S value (Table 2); thus, no charge separation can take place. Accordingly, only $^3C_{60}$*−DPAF is formed via intersystem crossing from $^1C_{60}$*−DPAF.

In PhCN, the reason the charge-separated state was observed as only a minor component compared with $^3C_{60}$*−DPAF is not clear. Contribution of C_{60}−^{1}DPAF* to the charge-separation process seemed to be minor; this reason is not revealed only from considering these energy diagrams.

For the mixture system of C_{60} with **A** or **B** (Figure 12B), intersystem crossing (k_{isc}) from $^1C_{60}$* to $^3C_{60}$* occurs prior to electron transfer from **A** or **B** (k_{et}), since $k_{isc} \gg k_{et}^S$[**A**] or k_{et}^S[**B**], when [**A**] and [**B**] are less than 5 mM.[23] Therefore, electron transfer takes place predominantly via $^3C_{60}$*.

Comparison with Other Organoamine Donor−*C_{60} Dyads.* The lifetime of the radical ion pair in the *N*,*N*-dimethylaniline (DMA)−C_{60} dyad with long spacers is quite long in polar solvents (τ_{IP} = ca. 250 ns).[7] Transient absorption spectra reported for the fused BBA−C_{60} dyad in the visible and near-IR regions indicated the formation of the BBA cation radical with an absorption peak at 800 nm; the τ_{IP} value of the BBA−C_{60} dyad was 250 ns in PhCN, which is slightly longer than that of C_{60}−DPAF in DMF.[8] However, C_{60}−DPAF in DMF showed temperature-dependent k_{CR} values, giving a chance to evaluate the coupling matrix element (V) and reorganization energy (λ).

Conclusion

We observed photoinduced intramolecular charge separation in C_{60}−DPAF via $^1C_{60}$*−DPAF in DMF; the lifetime of $C_{60}^{\bullet-}$-DPAF$^{\bullet+}$ was 150 ns. Such a relatively long lifetime was reasonable on the basis of the small reorganization energy evaluated by the temperature-dependent k_{CR} values. In PhCN, although efficient charge separation takes place, $C_{60}^{\bullet-}$-DPAF$^{\bullet+}$ was not clearly recognized, probably because the lifetime of $C_{60}^{\bullet-}$-DPAF$^{\bullet+}$ is too short for it to be observed by the nanosecond transient absorption method. In toluene, charge separation does not occur, because the energy level of $C_{60}^{\bullet-}$-DPAF$^{\bullet+}$ is higher than that of $^1C_{60}$*−DPAF.

Acknowledgment. The present work was partly supported by a Grant-in-Aid for Scientific Research from the Ministry of Education, Science, Sports and Culture of Japan (Nos. 10207202, 11740380, and 12875163). We are also grateful for financial support by Core Research for Evolution Science and Technology (CREST) of the Japan Science and Technology Corp.

Supporting Information Available: Figure showing the nanosecond transient absorption spectra of C_{60} in the presence of 2-aminofluorene and time profiles of absorbance at 740 and 1080 nm. This material is available free of charge via the Internet at http://pubs.acs.org.

References and Notes

(1) Guldi, D. M.; Kamat, P. V. In *Fullerenes, Chemistry, Physics and Technology*; Kadish, K. M., Ruoff, R. S., Eds.; Wiley-Interscience: New York, 2000; pp 225−281.

(2) Maggini, M.; Guldi, D. M. In *Molecular and Supramolecular Photochemistry*; Ramamurthy, V., Schanze, K. S., Eds.; Marcel Dekker: New York, 2000; Vol. 4, pp 149−196.

(3) (a) Arbogast, J. W.; Foote, C. S.; Kao, M. *J. Am. Chem. Soc.* **1992**, *114*, 2277. (b) Biczok, L.; Linschitz, H. *Chem. Phys. Lett.* **1992**, *195*, 339. (c) Nonell, S.; Arbogast, J. W.; Foote, C. S. *J. Phys. Chem.* **1992**, *96*, 4169. (d) Ito, O. *Res. Chem. Intermed.* **1997**, *23*, 389.

(4) Martin, N.; Sánchez, I.; Illescas, B.; Pérez, I. *Chem. Rev.* **1998**, *98*, 2527.

(5) Wasielewski, M. R. *Chem. Rev.* **1992**, *92*, 435.

(6) (a) Imahori, H.; Ozawa, S.; Uchida, K.; Takahashi, M.; Azuma, T.; Ajavakom, A.; Akiyama, T.; Hasegawa, M.; Taniguchi, S.; Okada, T.; Sakata, Y. *Bull. Chem. Soc. Jpn.* **1999**, *72*, 485. (b) Hirayama, D.;

Yamashiro, T.; Takimiya, K.; Aso, Y.; Otsubo, T.; Norieda, H.; Imahori, H.; Sakata, Y. *Chem. Lett.* **2000**, 570.

(7) (a) Williams, R. M.; Zwier, J. M.; Verhoeven, J. M. *J. Am. Chem. Soc*. **1995**, *117*, 4093. (b) Williams, R. M.; Koeberg, M.; Lawson, J. M.; An, Y.-Z.; Rubin, Y.; Paddon-Row: M. N.; Verhoeven, *J. Org. Chem.* **1996**, *61*, 5055.

(8) Komamine, S.; Fujitsuka, M.; Ito, O.; Morikawa, K.; Miyata, T.; Ohno, T. *J. Phys. Chem. A* **2000**, *104*, 11497.

(9) Chiang, L. Y.; Padmawar, P. A.; Canteenwala, Tan, T. L.-S.; He, G. S.; Kannan, R.; Vaia, R.; Lin, T.-C.; Zheng, Q.; Prasad, P. N. *Chem. Commun.* **2002**, 1854.

(10) (a) Fujitsuka, M.; Masuhara, A.; Kasai, H.; Oikawa, H.; Nakanishi, H.; Ito, O.; Yamashiro, Y.; Aso, Y.; Otsubo, T. *J. Phys. Chem. B* **2001**, *105*, 9930. (b) Fujitsuka, M.; Ito, O.; Yamashiro, T.; Aso, Y.; Otsubo, T. *J. Phys. Chem. A* **2000**, *104*, 4876. (c) Fujitsuka, M.; Matsumoto, K.; Ito, O.; Yamashiro, T.; Aso, Y.; Otsubo, T. *Res. Chem. Intermed.* **2001**, *27*, 73.

(11) Rehm, D.; Weller, A. *Isr. J. Chem*. **1970**, *8*, 259.

(12) Allemand, P. M.; Koch, A.; Wudl, F.; Rubin, Y.; Diederich, F.; Alvarez, M. M.; Anz, S. J.; Whetten, R. L. *J. Am. Chem. Soc*. **1991**, *113*, 1050.

(13) Hung, R. R.; Grabowski, J. J. *J. Phys. Chem*. **1991**, *95*, 6073.

(14) Senior, R. J.; Szarka, A. Z.; Smith, G. R.; Hochstrasser, R. M. *Chem. Phys. Lett*. **1991**, *185*, 179.

(15) Heath, G. A.; McGrady, J. E.; Martin, R. L. *J. Chem. Soc., Chem. Commun.* **1992**, 1272.

(16) (a) Steren, C. A.; von Willigen, H.; Biczok, L.; Gupta, N.; Linschitz, H. *J. Phys. Chem*. **1996**, *100*, 8920. (b) Alam, M. M.; Watanabe, A.; Ito, O. *Bull. Chem. Soc. Jpn*. **1997**, *70*, 1833.

(17) Yahata, Y.; Sasaki, Y.; Fujitsuka, M.; Ito, O. *J. Photosci.* **1999**, *6*, 117.

(18) Ito, O.; Sasaki, Y.; Yoshikaw, Y.; Watanabe, A. *J. Phys. Chem*. **1995**, *99*, 9838.

(19) D'Souza, F.; Deviprasad, G. R.; El-Khouly, M. E.; Fujitsuka, M.; Ito, O. *J. Am. Chem. Soc*. **2001**, *123*, 5277.

(20) Konoshi, T.; Fujitsuka, M.; Ito, O. *Chem. Lett.* **2000**, 202.

(21) (a) Marcus, R. A. *Annu. Rev. Phys. Chem.* **1964**, *15*, 144. (b) Marcus, R. A.; Sutin, N. *Biochim. Biophys. Acta* **1985**, *811*, 265. (c) Marcus, R. A. *Angew. Chem., Int. Ed. Engl.* **1993**, *32*, 1111.

(22) Imahori, H.; Tamaki, K.; Guldi, D. M.; Luo, C.; Fujitsuka, M.; Ito, O.; Sakata, Y.; Fukuzumi, S. *J. Am. Chem. Soc*., **2001**, *123*, 2607.

(23) (a) Ma. B.; Sun. Y. P. *J. Chem. Soc., Perkin Trans. 2* **1996**, 2157. (b) Watanabe, A.; Ito, O.; Saito, H.; Watanabe, M.; Koishi, M. *J. Chem. Soc., Chem. Commun*. **1996**, 117.